iScience

CellPress

Article

Cell Membrane and Electron Transfer Engineering for Improved Synthesis of Menaquinone-7 in *Bacillus subtilis*

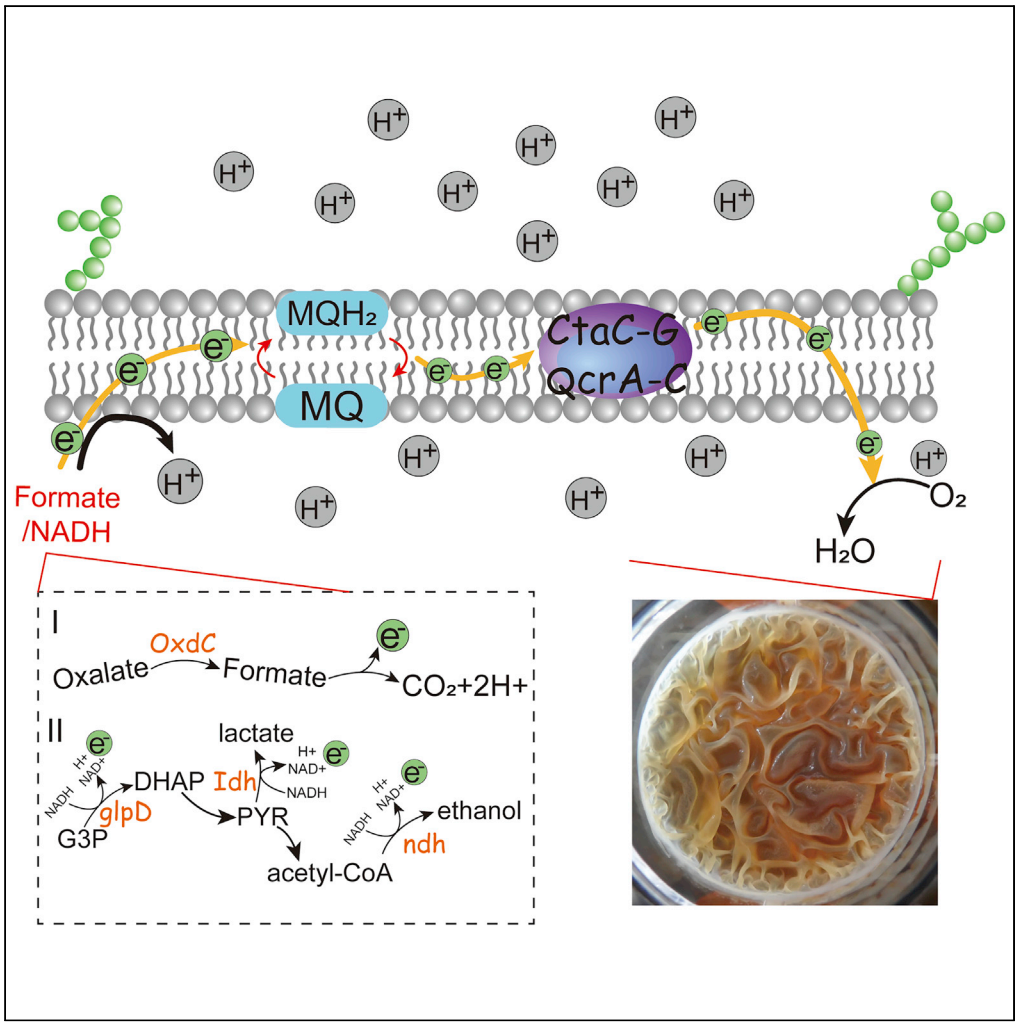

Shixiu Cui, Hongzhi Xia, Taichi Chen, ..., Jianghua Li, Guocheng Du, Long Liu

longliu@jiangnan.edu.cn

HIGHLIGHTS

Transcriptome analysis shows the relationship between biofilm and MK-7 synthesis

Electron transfer significantly affects the synthesis of MK-7

Oxalate decarboxylase OxdC plays a role in electron generation and MK-7 synthesis

Cui et al., iScience *23*, 100918 March 27, 2020
https://doi.org/10.1016/j.isci.2020.100918

iScience

CellPress

Article

Cell Membrane and Electron Transfer Engineering for Improved Synthesis of Menaquinone-7 in *Bacillus subtilis*

Shixiu Cui,[1,2,4] Hongzhi Xia,[3,4] Taichi Chen,[1,2] Yang Gu,[1,2] Xueqin Lv,[1,2] Yanfeng Liu,[1,2] Jianghua Li,[1,2] Guocheng Du,[1,2] and Long Liu[1,2,5,*]

SUMMARY

The formation of biofilm facilitates the synthesis of valuable natural product menaquinone-7 (MK-7) in static culture of *Bacillus subtilis*, whereas the essential role and mechanism of biofilm in MK-7 synthesis have not been revealed. Herein, comparative transcriptomics show that the formation of biofilm affected MK-7 synthesis by changing the transcription levels of signal receptor (BSU02010), transmembrane transporter (BSU29340, BSU03070), and signal transduction (BSU02630). Moreover, we also found that oxalate decarboxylase OxdC has an important effect on electron generation and MK-7 synthesis, when the transcriptional level of NADH dehydrogenase decreases in static culture. Our results revealed that cell membrane and electron transfer are important factors in promoting MK-7 synthesis.

INTRODUCTION

As a highly valuable vitamin K2, menaquinone-7 (MK-7) is a polyene compound consisting of 2-methyl-1,4-naphthoquinone ring structure with a side chain of 7 isoprene units (Berenjian et al., 2015). It was reported that MK-7 is the component of microbial plasma membrane and plays an important role in electron transport and oxidative phosphorylation (Berenjian et al., 2013). Owing to the good bioavailability, MK-7 functions in protecting human health (Sato et al., 2012), such as prevention of osteoporosis (Iwamoto, 2014), arterial calcification, cardiovascular, and Parkinson diseases (Groberet al., 2014; Ravishankar et al., 2015).

In the past decades, many studies have focused on improving the production of MK-7 by microbial fermentation (Berenjian et al., 2011; Mahanama et al., 2011; Wu and Ahn, 2011). For example, by optimizing medium nutrients the maximum concentration of MK-7 reached 62.32 mg/L (Berenjian et al., 2011); the fed-batch culture modes were then adopted to increase the titer of MK-7 by 40% to 86.48 mg/L (Berenjian et al., 2012). Furthermore, Yang et al. (2019) divided the MK-7 synthesis pathways into four modules and overexpressed several key genes including *menA*, *dxs*, *dxr*, *yacM-yacN*, and *glpD*, resulting in the increase of MK-7 titer to 69.5 mg/L. It was noteworthy that static culture was likely to be beneficial to MK-7 production, which may be attributed to the biofilm formation in static culture (Berenjian et al., 2013). As well known, biofilm is an assemblage of tightly associated bacteria encapsulated by a self-produced extracellular matrix (Mielich-Suss and Lopez, 2015) and creates favorable conditions for sustainable survival in the natural environment (Cairns et al., 2014). Interestingly, Mahdinia et al. (2018) used the biofilm reactor with four different types of plastic composite carriers to produce MK-7 and increased the MK-7 titer by 2.3-fold to 28.7 mg/L. However, the specific role and mechanism of biofilm in the synthesis of MK-7 have not been revealed at genetic level, and this limits the possibility of further increasing MK-7 production.

To illuminate the intrinsic connections between the biofilm formation and MK-7 production, *Bacillus subtilis*, a Gram-positive model microorganism that has been widely used in the production of nutraceuticals and enzymes (Song et al., 2015), was selected as the host in this work. First, by knocking out the biofilm-forming genes *epsA-C*, *tasA*, *sinI*, *yuaB*, and *ftsH*, we verified that biofilms have significant effects on MK-7 synthesis. Then, the comparative transcriptomics analysis of the strains in shake culture and static culture was performed, and the results showed that the expression of genes involved in biological process, molecular function, and cellular component was upregulated. In particular, some differential genes were related to the membrane components, such as transmembrane transporter (BSU29340, BSU03070), and the expression level of eight NADH dehydrogenases was downregulated. Moreover, sodium dodecyl

[1]Key Laboratory of Carbohydrate Chemistry and Biotechnology, Ministry of Education, Jiangnan University, Wuxi 214122, China

[2]Key Laboratory of Industrial Biotechnology, Ministry of Education, Jiangnan University, Wuxi 214122, China

[3]Richen Bioengineering Co., Ltd, Nantong 226000, China

[4]These authors contributed equally

[5]Lead Contact

*Correspondence: longliu@jiangnan.edu.cn

https://doi.org/10.1016/j.isci.2020.100918

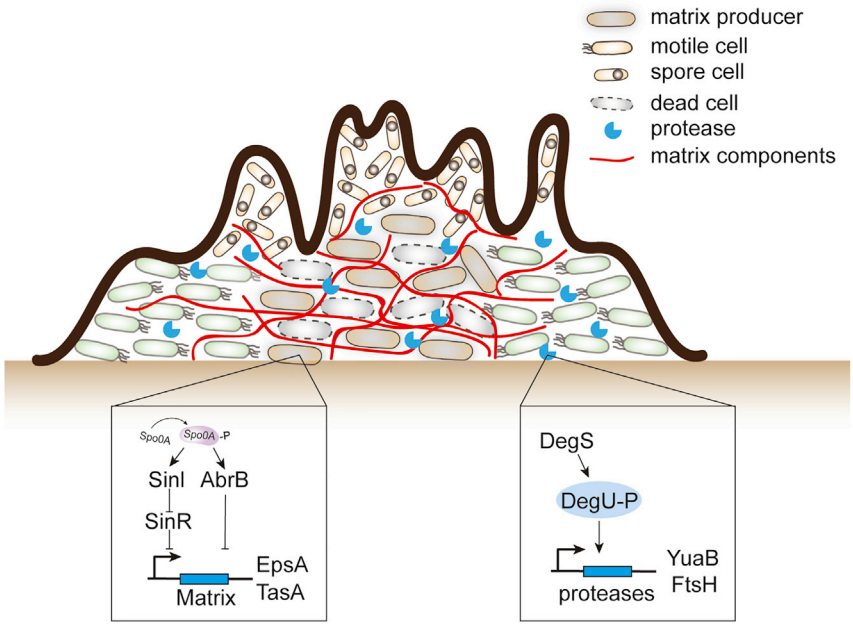

Figure 1. Schematic Diagram of Cross-Sectional Structure of Biofilm

Different types of cell subpopulations co-exist and exhibit different temporal and spatial distribution patterns. The genetic program associated with cell differentiation is shown in the box, and the genes associated with each differentiation process are located within a specific framework. The expression of *yqxM-tasA* operons is controlled by regulatory repressor SinI and anti-repressor protein SinR. The major proteinaceous component of matrix yuab and ftsh is controlled by DegS-DegU two-component regulation system.

sulfate polyacrylamide gel electrophoresis (SDS-PAGE) and NADH content analysis showed that the oxalate-decarboxylase (OxdC) was abundantly expressed and could provide a large number of electrons through the delivery of cytochrome *c* and MK-7 in static culture. Finally, combinatorial overexpression of cell membrane protein *tatAD-CD* and menaquinol-cytochrome C reductase *qcrA-C* significantly increased the titer of MK-7 from 200 to 310 mg/L in a 15-L bioreactor. All these results demonstrate that biofilm can promote the synthesis of MK-7 of *B. subtilis* by modulating the cell membrane components and electron transfer.

RESULTS

Biofilm Significantly Affects the Synthesis of MK-7 in *B. subtilis*

Biofilm is a dynamic community composed of at least three cell types including matrix-producing cells, motile cells, and sporulation cells (Cairns et al., 2014). These cells are encapsulated by the matrices including exopolysaccharides (EPS), fibrils formed by secreted protein (TasA), and extracellular DNA (Figure 1). In *B. subtilis*, the EPS and TasA are encoded by the *epsA-C* operon and *yqxM-tasA* operon, respectively (Romero et al., 2010; Diehl et al., 2018). As shown in Figure 2A, deletion of *epsA-C* and *yqxM-tasA* operons inhibited the formation of *B. subtilis* biofilm in static culture, resulting in a significant decrease of specific MK-7 titer from 1.6 μg/mg of *B. subtilis* 168 to 1.2 μg/mg and 0.65 μg/mg, respectively. Compared with the *B. subtilis* 168, the biomass of cells with deletion of *epsA-C* and *yqxM-tasA* operons increased by 44% and 35%, respectively (Figure 2B). Considering that the expression of *yqxM-tasA* operons is controlled by the regulatory repressor SinI and anti-repressor protein SinR (Brandaet al., 2006; Chu et al., 2006), we deleted *sinI* gene and found that the specific MK-7 titer decreased from 1.60 μg/mg to 0.46 μg/mg and the biomass increased from 14.3 g/L to 17.5 g/L (Figures 2A and 2B). Moreover, YuaB, the major proteinaceous component of matrix, is essential to form a water-repellent surface layer in the biofilm by self-assembly (Kobayashi and Iwano, 2012; Liu et al., 2017). Knockout of the gene *yuaB* inhibited the formation of biofilm and the specific MK-7 titer decreased by 37.5% to 1 μg/mg (Figures 2A and 2B). Besides, the membrane-bound protease FtsH is also important for biofilm formation (Yepes et al., 2012), and here the deletion of *ftsH* gene decreased the specific MK-7 titer from 1.60 μg/mg to 0.69 μg/mg (Figures 2A and 2B).

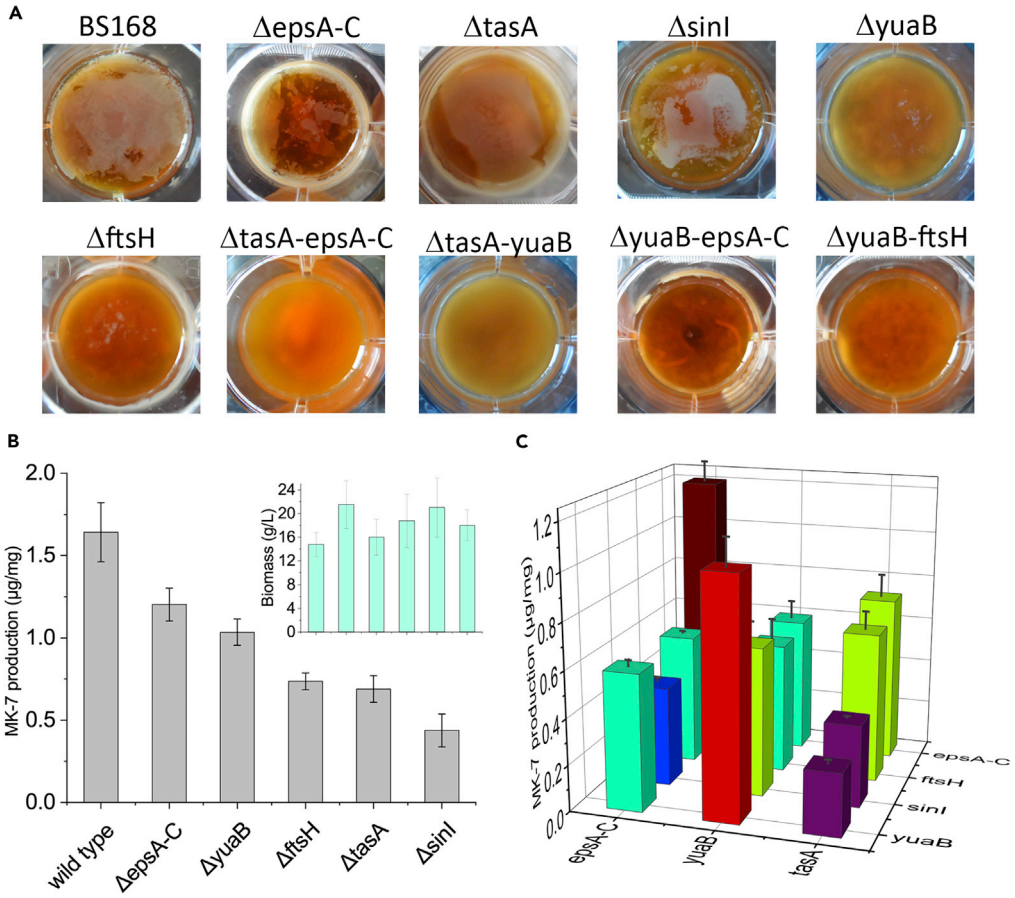

Figure 2. The Relationship between Biofilm Formation and MK-7 Titer

(A) The morphological changes of the biofilm when the key genes were knocked out, including single and double knockout of key genes.

(B) The specific titer of MK-7 when biofilm formation genes were knocked out. The small image in the upper right corner is biomass.

(C) Effect of double deletion of key genes in biofilm formation on specific titer of MK-7. All experiments were independently carried out at least three times, and the results were expressed as mean ± standard deviation (SD).

In addition, the combinatorial deletion of these genes significantly decreased the biofilm formation and MK-7 synthesis (Figure 2A). In particular, when *yqxM-tasA* operon and *yuaB* were knocked out simultaneously, the synthesis of extracellular polysaccharide and protein was blocked and almost no biofilm was formed (Figure 2A), resulting in a significant decrease of specific MK-7 titer to only 0.25 μg/mg (Figure 2C), whereas little influence on cell growth (Figure S1). Simultaneous deletion of *tasA* and *yuaB* genes may change the mechanical strength of the matrix, resulting in a more homogeneous pattern of cell death. On the other hand, disassembly of bacterial biofilm has a negative effect on the attachment of bacterial cell wall and extracellular matrix to affect cell growth (Mielich-Suss and Lopez, 2015). The above results indicate that biofilm formation was related with MK-7 synthesis and the inhibition of biofilm formation can significantly reduce MK-7 synthesis.

Comparative Transcriptomics Analysis of *B.subtilis* Strains in Static and Shake Culture

The comparative transcriptomics analysis was performed to analyze the changes of global gene expression in MK-7 synthesis by static culture and shake culture. The transcriptomics data have been deposited in the NCBI Sequence Read Archive (SRA) (accession number: PRJNA599448). Table S1 shows the statistical summary of the transcriptome sequencing data, and the data from all differentially expressed genes in *B. subtilis* 168 were used for systematic cluster analysis to gain insight into the differences between the

transcriptomes of static and shake culture. The heatmap suggests that the selected differential genes are clearly consistent (Figure S2).

The comparative transcriptomic results show that the expression of most genes in glycolysis pathway, pentose phosphate pathway, and shikimic acid pathway was upregulated in static culture, whereas the expression of genes in 2-C-methyl-D-erythritol-4-phosphate (MEP) pathway and MK-7 synthesis pathway was downregulated in static culture (Figure 3A). The quantitative reverse transcription polymerase chain reaction (qRT-PCR) was also used to verify the result of comparative transcriptomics analysis, and both results were consistent (Figure S3). That is to say, static culture could upregulate the central metabolic pathway genes and enhance the chorismic acid synthesis. In particular, compared with the shake culture, the expression levels of most NADH dehydrogenases, except *glpD*, *yumB*, and *ahpF*, significantly decreased in the static culture (Figure 3B). Further investigation of the expression of the other dehydrogenases showed that the expression of nearly half of the dehydrogenases was upregulated (Figure 3C). In addition, the expression levels of various amino acid dehydrogenases such as *ycgM*, *gcvpA*, *dhaS*, *bcd*, *ald*, *asd*, *hisD*, *tyrA*, and *gudB* increased. These results indicate that the central metabolic pathways and amino acid metabolism were promoted in static culture.

To systematically analyze the effect of differential genes on MK-7 synthesis, we classified them by Volcano map and Veen diagram and a total of 2,093 differentially expressed genes were obtained (Figure 4A). Compared with the shake culture, the expression levels of 1,281 genes were upregulated (Table S2) and 812 genes were downregulated (Table S3) in static culture. As shown in Figure 4B, 3,919, 3,973, 3,586, and 3,581 transcripts were detected in BS168 static-1, BS168 static-2, BS168 shake-1, and BS168 shake-2, respectively. There were 3,345 transcripts common to all the samples. Filtering analysis, Gene Ontology (GO) functional annotation, and Kyoto Encyclopedia of Genes and Genomes (KEGG) pathway analysis were carried out, and the results show that GO functional annotation classified the differential genes into three categories: molecular function, cellular component, and biological process, whereas KEGG pathway analysis classified the differential genes into six categories with the most significant difference in metabolism category (Figures 4C and 4D). To determine the gene functional classes in static culture, we carried out a homology-based annotation specifically for all the 2,093 differentially expressed genes, and GO terms related to the dataset are shown in Table S4. Significant differences were found in expression of genes involved in biological process, molecular function, and cellular component (Figure 4C). In particular, the changes were obviously in the membrane component (GO:0006810, GO:0017000, GO:0008125, GO:0031224, GO:0051234), indicating that cell membrane could affect MK-7 synthesis. Moreover, the enrichment of terms related to biotic stress and oxidative stress were distinct (GO:0043207, GO:0006979). In addition, enrichment of gene functions related to transporter and transcription were observed (GO:0071944, GO:0051234, GO:0006139), which possibly generated a response of the external stimuli and transmit signals into cells to regulate gene expression. In general, compared with shake culture, the enrichment analysis of GO terms indicates that the differential genes were mainly related to signal transduction and membrane components (Figure 4C), indicating that the unknown signal transduction generated in static culture may lead to changes in membrane components to regulate the synthesis of MK-7.

The set of 2,093 differentially expressed genes was mapped onto KEGG pathways in *B. subtilis* 168 (Table S5), highlighting the involvement of amino acid, cofactors, and vitamin metabolism as well as the transmembrane transport. Amino acid metabolism in static culture was significantly different from that in shake culture. The transcripts of synthetases involved in amino acids were upregulated, except tryptophan and threonine dehydrogenase, indicating that amino acid synthesis may affect the synthesis of MK-7. Two other important pathways, "Two component system" (ko02020) and "ABC transporters" (ko02010), were also found to be upregulated in static culture (Figure 4D). PhoD (alkaline phosphatase D), alkaline phosphatase synthesis sensor protein PhoR, and phosphate transport system substrate-binding protein PstS, associated with the transfer of phosphate groups were all upregulated in static culture. Additionally, several transcripts from *ydfI* (transcriptional regulator), *phoAB* (alkaline phosphatase), *cheY* (chemotaxis protein), *ssuA* (sulfonate transport system substrate-binding protein), *mntB* (manganese/zinc/iron transport system ATP- binding protein), *cysC* (adenylyl sulfate kinase), and *ytrB* (acetoin utilization transport system ATP-binding protein) were also upregulated in static culture. All these genes have been reported to be involved in response to several stresses, such as phosphate limitation (Antelmann et al., 2000) and metal ion stress (Que and Helmann, 2000). The synthesis of secondary metabolites (ko01110) also had significant differences, including

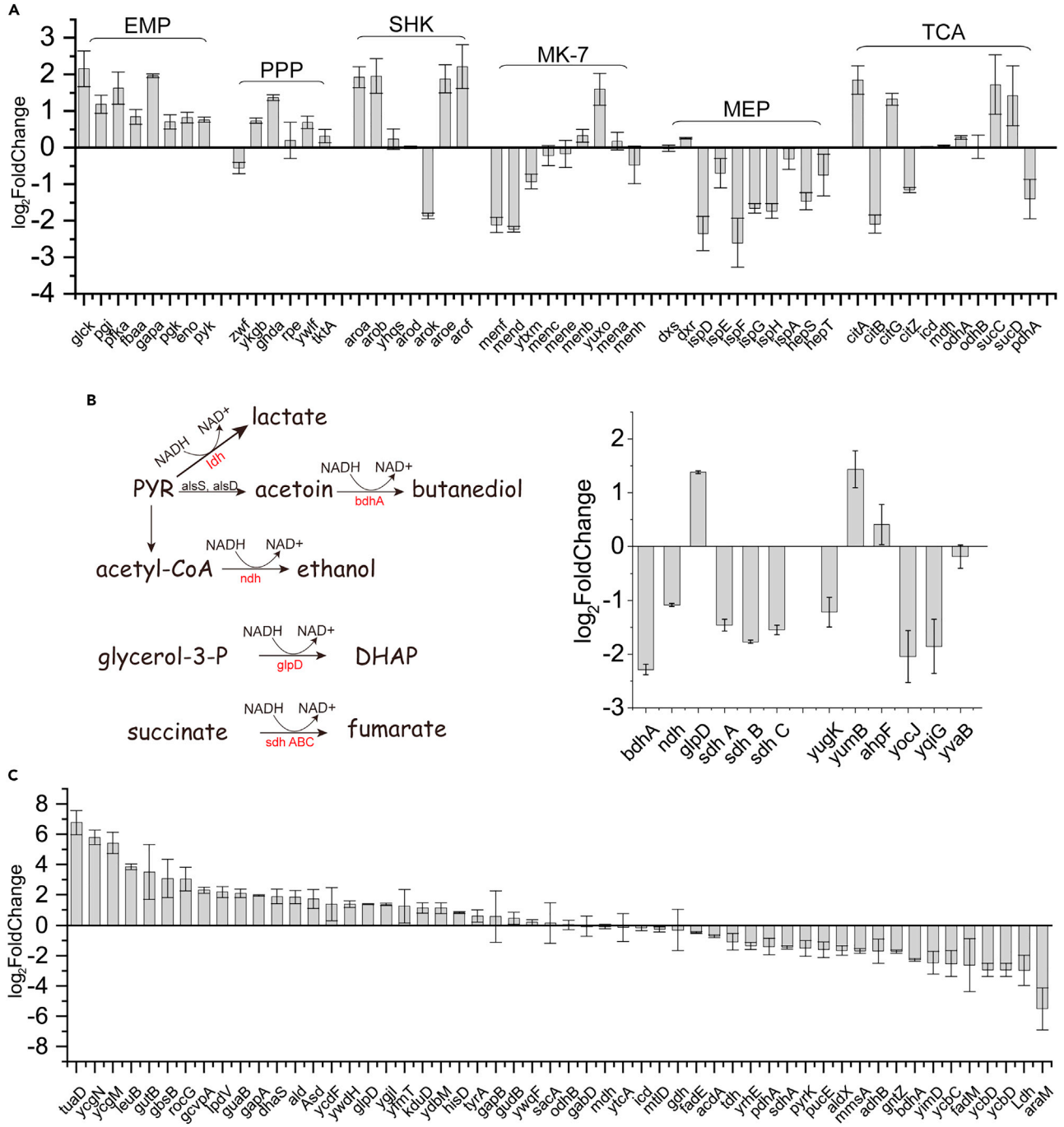

Figure 3. The Expression Level of MK-7 Synthesis Related Genes in Static Culture Compared with Shake Culture

(A) Expression levels of genes involved in MK-7 synthesis, including glycolysis pathway (EMP), pentose phosphate pathway (PPP), shikimic acid (SHK) pathway, MK-7 pathway, 2-C-methyl-D-erythritol-4-phosphate (MEP) pathway, and tricarboxylic acid cycle (TCA).

(B) Left: catalytic reaction of NADH reduction in cells, including L-lactate dehydrogenase (ldh), (R,R)-butanediol dehydrogenase (bdha), NADH dehydrogenase (ndh), aerobic glycerol-3-phosphate dehydrogenase (glpD), and succinate dehydrogenase flavoprotein (sdhABC). Right: expression level of NADH dehydrogenase in static culture, compared with shake culture; positive numbers mean upregulation; negative numbers mean downregulation.

(C) Expression level of most dehydrogenases of cells in static culture, including various amino acid dehydrogenases. All experiments were independently carried out at least three times, and the results were expressed as mean ± standard deviation (SD).

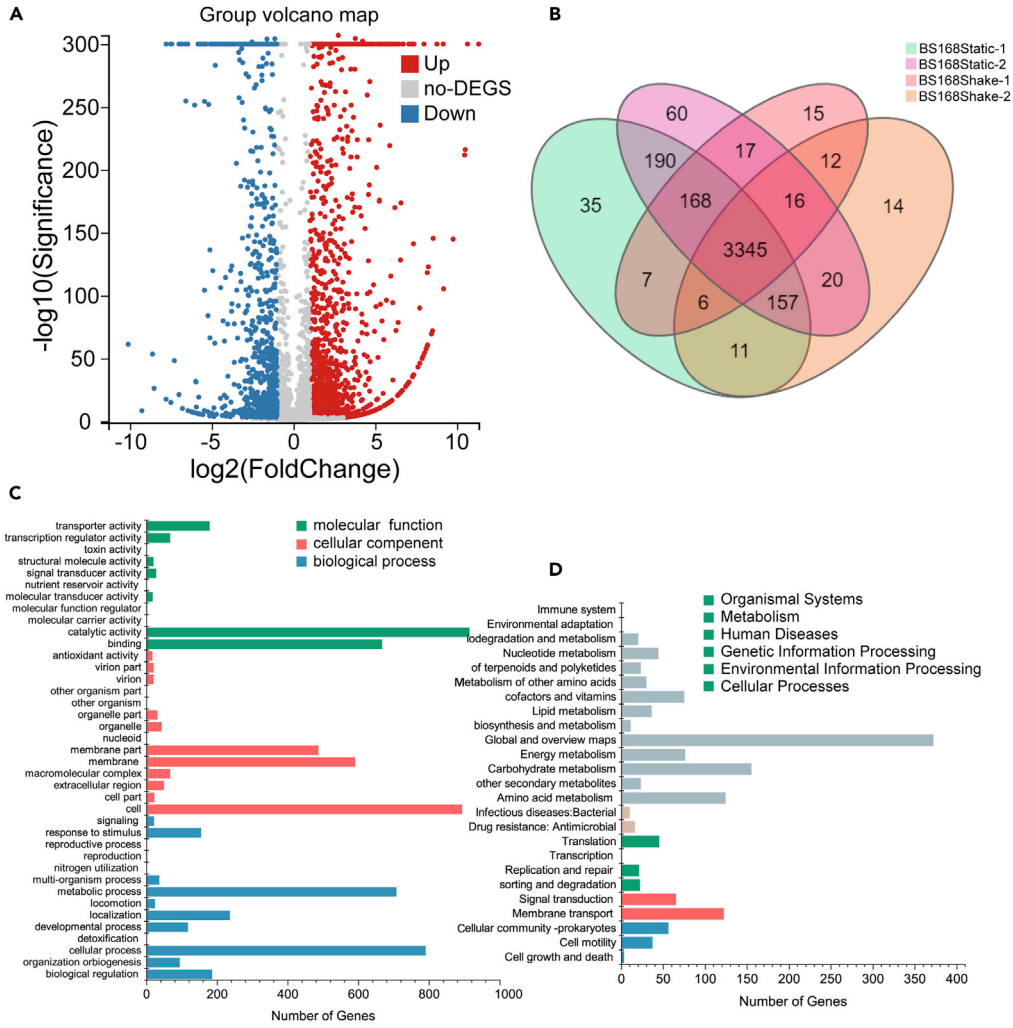

Figure 4. TranscriptomicsAnalysis of Differences between Shake Culture and Static Culture

(A) Volcanic maps show differentially expressed genes between groups. Red dots indicate upregulated genes and blue dots indicate downregulated genes.

(B) Venn shows differentially expressed genes between each sample.

(C) Gene Ontology (GO) functional analysis of differential genes. According to gene function, it can be divided into three categories: molecular function, cellular components, and biological processes. The obvious differences in membrane part and catalytic activity.

(D) Kyoto Encyclopedia of Genes and Genomes (KEGG) pathway analysis of functions of differential genes. The most significant differences in cell metabolism category, include cofactors and vitamins metabolism, energy metabolism, and amino acid metabolism. All experiments were independently carried out at least three times, and the results were expressed as mean ± standard deviation (SD).

coenzymes and vitamins, such as biotin (ko00780), thiamine (ko00730), and folate (ko00790). Taken together, these results indicate that compared with shake culture, static culture had significant effects on signal transduction, amino acid metabolism, and secondary metabolite synthesis.

Overexpression of Differential Genes in *B. subtilis* 168 and the Engineered Strain BS20

According to the above analysis, influence of the differential genes on the synthesis of MK-7 by the static culture of *B. subtilis* 168 was first examined. Table S6 shows the selected differential genes, which are involved in signal transduction, transmembrane transport, and oxidative phosphorylation. According to the influence of differential gene overexpression on biofilm formation, these genes can be divided into two groups, promoting biofilm formation group and inhibiting biofilm formation group. The former group

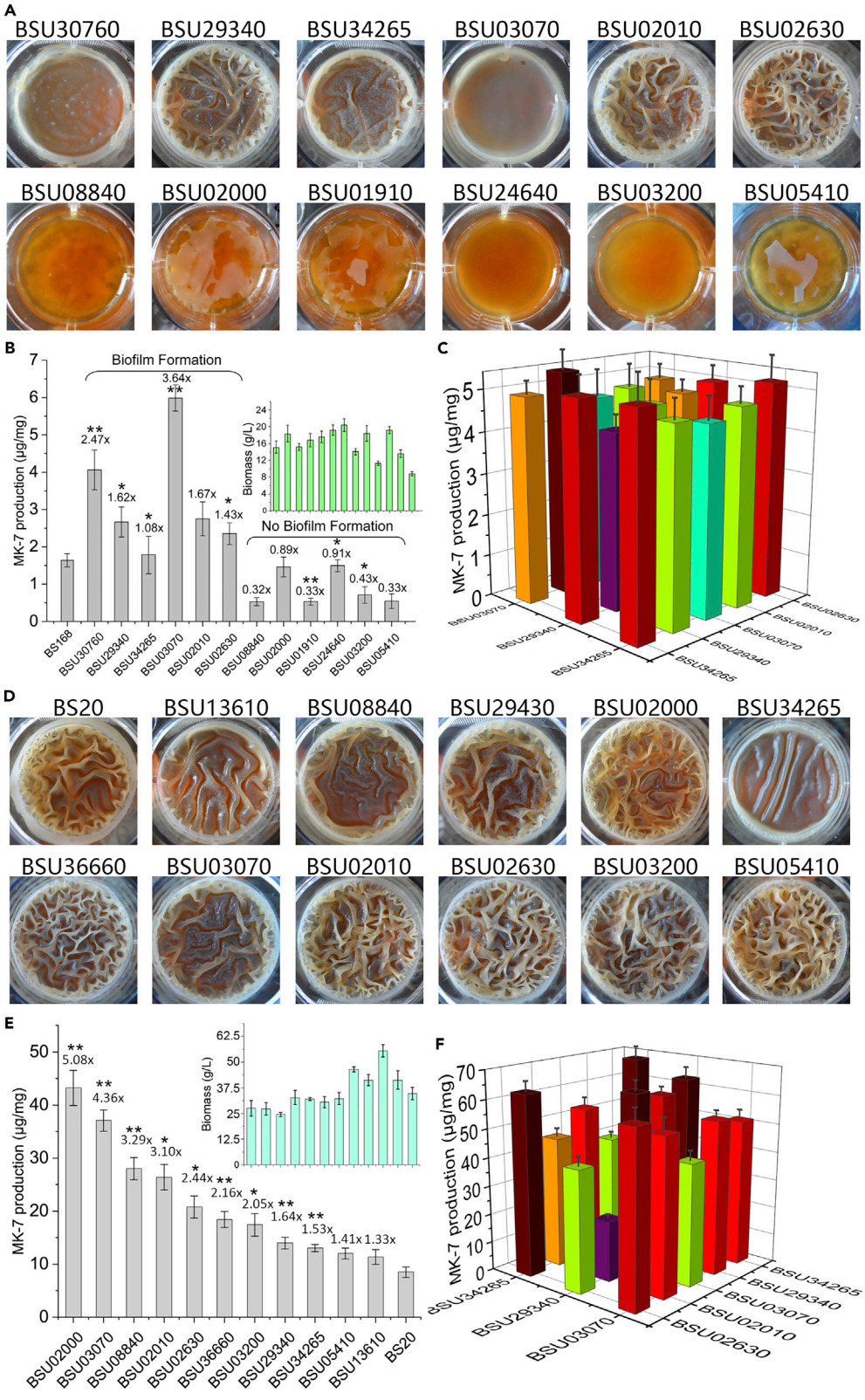
A
BSU30760
BSU29340
BSU34265
BSU03070
BSU02010
BSU02630
BSU08840
BSU02000
BSU01910
BSU24640
BSU03200
BSU05410
B
Biofilm Formation
No Biofilm Formation
MK-7 production (μg/mg)
Biomass (g/L)
BS168
BSU30760
BSU29340
BSU34265
BSU03070
BSU02010
BSU02630
BSU08840
BSU02000
BSU01910
BSU24640
BSU03200
BSU05410
C
MK-7 production (μg/mg)
D
BS20
BSU13610
BSU08840
BSU29430
BSU02000
BSU34265
BSU36660
BSU03070
BSU02010
BSU02630
BSU03200
BSU05410
E
MK-7 production (μg/mg)
Biomass (g/L)
BSU02000
BSU03070
BSU08840
BSU02010
BSU02630
BSU36660
BSU03200
BSU29340
BSU34265
BSU05410
BSU13610
BS20
F
MK-7 production (μg/mg)

Figure 5. Overexpression of Differentially Expressed Genes in *B. subtilis* 168 and BS20

(A) Overexpression of differentially expressed genes in *B. subtilis* 168 and differences in biofilm morphology.

(B) Effect of overexpression of differential genes on the titer of MK-7 in *B. subtilis* 168. The small image in the upper right corner is biomass.

(C) Effect of combinatorial overexpression of differential genes on the titer of MK-7 in *B. subtilis* 168.

(D) Overexpression of differentially expressed genes in the engineered strain BS20 and differences in biofilm morphology.

(E) Effect of overexpression of differential genes on the titer of MK-7 in BS20. The small image in the upper right corner is biomass.

(F) Effect of combinatorial overexpression of differential genes on the titer of MK-7 in BS20. All experiments were independently carried out at least three times, and the results were expressed as mean ± standard deviation (SD). *$p < 0.05$ and **$p < 0.01$, respectively.

mainly includes the genes BSU30760, BSU29340, BSU34265, BSU03070, BSU02010, and BSU02630. When these genes were overexpressed by the strong constitutive promoter P_{43}, the cells concentrated on the surface of medium, and a large amount of biofilm formed compared with *B. subtilis* 168 (Figure 5A). The specific MK-7 titer was increased by 45% and 160% when BSU02630 and BSU30760 were overexpressed in *B. subtilis* 168, respectively. Especially when overexpressing BSU03070, the specific MK-7 titer was increased to 6.0 μg/mg, 3.75-fold that of *B. subtilis* 168 (Figure 5B). In addition, there were significant differences in biofilm morphology among strains overexpressing BSU30760, BSU29340, BSU34265, BSU03070, BSU02010, and BSU02630. The surface of the biofilm in the strains overexpressing BSU30760 or BSU03070 was smooth without wrinkles, whereas the overexpression of other genes generated a large number of wrinkles. Strangely, the biofilm formed by BSU34265 overexpression was not as smooth as the other biofilms, and a large number of particles appeared on the surface. However, the cells overexpressing BSU08840, BSU02000, BSU01910, BSU24640, BSU03200, and BSU05410 settled at the bottom of the medium without biofilm formation (Figure 5A), and the specific MK-7 titer decreased from 1.6 μg/mg to 0.5–1.45 μg/mg. Moreover, overexpression of these genes, except BSU24640 and BSU02000, significantly decreased the biomass (Figure 5B). Finally, the constitutive strong promoter P_{43} was used for overexpression of the genes that can promote biofilm formation, and we investigated 15 arrays containing different combinations of genes (Figure S4). Figure 5C shows that the titer of MK-7 did not further increase, and for co-overexpression of BSU29340 and BSU34265, the biomass of cells decreased from 14.3 to 10 g/L (Figure S5).

In a recent work, we have developed a bifunctional quorum-sensing system in *B. subtilis* 168 to engineer the synthesis modules of MK-7 and obtained a recombinant strain BS20, which can produce 360 mg/L MK-7 in shaker flask and 200 mg/L MK-7 in 15-L bioreactor (Cui et al., 2019). In this work, we further verified the influence of differential genes on MK-7 synthesis in the engineered strain BS20 in the static culture. It was found that different from *B. subtilis* 168, the overexpression of differential genes BSU13610, BSU08840, BSU29430, BSU02000, BSU34265, BSU36660, BSU03070, BSU02010, BSU02630, BSU03200, and BSU05410 in BS20 can promote to form a large amount of biofilms (Figure 5D), and the biofilms are more wrinkled. Moreover, the specific MK-7 titer of the strains overexpressing the above genes was significantly improved compared with BS20, with an increase ranging from 20% to 400% (Figure 5E). Specifically, the synthesis of MK-7 increased from 9.02 to 42.5 μg/mg in the strain overexpressing BSU02000. In addition, compared with the biomass of *B. subtilis* 168, the biomass of strain BS20 increased by nearly 2–3 times and reached a maximum of 50 g/L (Figures 5B and 5E). Finally, the specific MK-7 titer was increased by 30%–50% by overexpression of differential genes in combination compared with that in single-gene overexpression. For example, in the strains co-expressing BSU34265 and BSU02630 or co-expressing BSU29340 and BSU03070, the specific MK-7 titer increased from 9.02 to 65 μg/mg and 58 μg/mg, respectively (Figure 5F). In summary, the signal transduction (BSU02000, BSU02630) and transmembrane transport (BSU34265, BSU29340, BSU03070) in the strain BS20 had significant effects on the synthesis of MK-7.

Electron Transfer Has Significant Effects on MK-7 Synthesis in *B. subtilis*

MK-7 plays an important role in electrons transport, oxidative phosphorylation, and sporulation (Berenjian et al., 2013). NADH is a molecule for donating electrons. Electrons are transported by MK-7 and cytochrome *c*, and finally oxygen acts as an electron acceptor to form water (Figure 6A). Besides, the cytochromes in *B. subtilis* 168 mainly include *ctaC-G* operator and *qcrA-C* operator (Yu et al., 1995; Lyons et al., 2012; Kolodkin-Gal et al., 2013; Qin et al., 2019). The expression level of *catC-G* and *qcrA-C* were

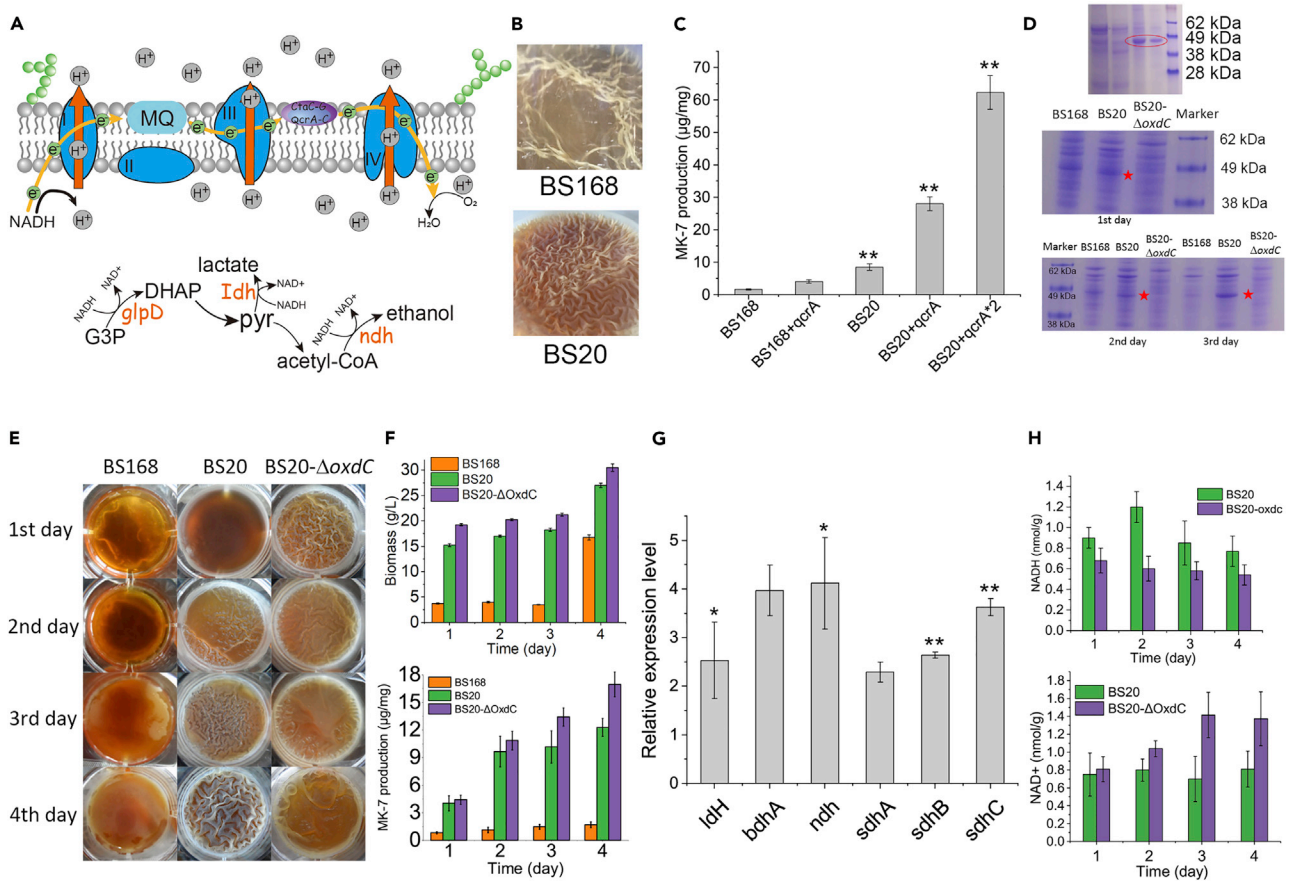

Figure 6. Effect of Electron Transfer Chain on the Synthesis of MK-7

(A) Schematic diagram of electron transfer chain in *B. subtilis* 168. Electrons are extracted under action of NADH dehydrogenase, and MK-7 and cytochrome *c* act as electron transport carriers, and finally electrons are delivered to oxygen to form water.

(B) Morphological differences in biofilms of *B. subtilis* 168 and BS20 overexpressed *qcrA-C* gene, respectively.

(C) Changes in MK-7 production when overexpression of *qcrA-C* gene in *B. subtilis* 168 and BS20. QcrA*2 means that there are two copies in BS20.

(D) Up: sodium dodecyl sulfate polyacrylamide gel electrophoresis (SDS-PAGE) analysis of fermentation broth protein components, and there is a very distinct band at 46 KDa. Down: the translation level of OxdC increases with the fermentation time, and SDS-PAGE verifies that *oxdC* was successfully knocked out in BS20.

(E) Comparison of biofilm morphology of *B. subtilis* 168 and BS20 (*oxdC* deletion).

(F) Changes in MK-7 production and cell biomass of BS20 with *oxdC* deletion.

(G) The relative expression levels of NADH dehydrogenase in the strain BS20 with *oxdC* deletion, and all the NADH dehydrogenases were upregulated when *oxdC* was knocked out.

(H) Changes in NADH and NAD content in the strain BS20 with *oxdC* deletion. All experiments were independently carried out at least three times and the results were expressed as mean ± standard deviation (SD). *$p < 0.05$ and **$p < 0.01$, respectively.

upregulated in static culture compared with that in shake culture (Figure S6). Moreover, to further verify the effect of cytochrome on MK-7 synthesis, we increased the expression level of menaquinol-cytochrome c reductase QcrA-C by the constitutive promoter P_{43} in *B. subtilis* 168 and BS20, respectively and found that there was a significant difference in biofilm morphology between the two strains. The overexpression of *qcrA-C* in *B. subtilis* 168 made the biofilm look smooth with a few wrinkles, and the specific MK-7 titer increased from 1.6 to 4.0 μg/mg, whereas the *qcrA-C* overexpression in BS20 made the biofilm form obvious wrinkles (Figure 6B), and the specific MK-7 titer increased from 9.02 to 28.0 μg/mg (Figure 6C). In addition, it was found that increasing the copy number of *qcrA-C* to 2 in BS20 can further improve the synthesis of MK-7 to 62.3 μg/mg, 2.23-fold that of single copy (Figure 6C). These results show that the increased expression of menaquinol-cytochrome reductase could significantly promote the synthesis of MK-7, indicating that more MK-7 can deliver more electrons, and MK-7 plays an indispensable role in electron transfer.

As mentioned above, NADH donates the electrons under action of NADH dehydrogenase and transfers electrons to the electron transport system (ETM) and pumps protons out of the cell. However, the expression of most NADH dehydrogenases was downregulated. Therefore, we speculate that there may be other processes that can donate large amounts of electrons. In order to confirm the above hypothesis, we analyzed the cellular proteins and found a very distinct band at 46 KDa using SDS-PAGE (Figure 6D). Combined with protein flight mass spectrometry, we revealed that the band was oxalate-decarboxylase (OxdC) (Figure S7), which requires Mn and O_2 to catalyze the conversion of oxalate to formate and CO_2 (Conter et al., 2019), and then formate is oxidized to CO2 and electrons by formatedehydratase (FdhD and YrhE) (Wilkset al., 2009; Glaser et al., 1995; Yang et al., 2015). Figure 6D shows that the expression of OxdC increases with the fermentation time. Next, we investigated the effect of deleting gene *oxdC* and blocking electron transport on the biofilm morphology and MK-7 synthesis in static culture. It was found that the knockout of *oxdC* in BS20 causes obvious changes in the morphology of biofilm. As shown in Figure 6E, the wrinkles of biofilm formed by the *oxdC* deletion strain BS20-Δ*oxdC* were less than that of BS20, whereas the biomass of BS20-Δ*oxdC* increased from 27.3 to 31.0 g/L (Figure 6F). The specific MK-7 titer also increased with fermentation time, and the specific MK-7 titer of BS20-Δ*oxdC* reached 17.5 μg/mg on the fourth day, 1.94-fold that of BS20 (Figure 6F). In addition, when *oxdC* was knocked out, the expression of NADH dehydrogenase *ldH*, *bdhA*, *ndH*, and *sdhA-C* was upregulated (Figure 6G), indicating that after *oxdC* knockout, NADH dehydrogenase compensates for the absence of electrons. These results indicate that the stability of electron transfer chain could increase the synthesis of MK-7. Moreover, the ratio of NADH/NAD^+ can characterize the rate of intracellular electrons extracted, and the NADH level in BS20 was higher than that of BS20-Δ*oxdC*, reaching 1.2 nmol/g on the second day, whereas the level of NAD^+ in BS20-Δ*oxdC* was higher than that of BS20 (Figure 6H), indicating that stable electron supply and transfer are important for the efficient synthesis of MK-7.

MK-7 Production by the Engineered *B. subtilis* Strain in 250 mL Flask and 15-L Bioreactor

Considering that signal transduction protein TatAD-CD (BSU02630) and methylphenol cytochrome *c*reductase QcrA-C can significantly promote the synthesis of MK-7, we co-expressed the *tatAD-CD* (BSU02630) and *qcrA-C* using P_{43} promoter in the engineered strain BS20 to study the effect of signal transduction and electron transfer on MK-7 synthesis in shake culture. Figure 7A shows that the MK-7 titer of strains BS20-T (*tatAD-CD* overexpression) and BS20-Q (*qcrA-C* overexpression) increased from 360 to 370 mg/L and 375 mg/L, respectively. The cell growth of BS20-T was increased and the maximum OD_{600} was 127% of BS20 (Figure 7B). To detect the substrate conversion rate, we detected the glucose content in static culture and shake culture. The results show that the consumption of glucose in shake culture was significantly higher than that in static culture (Figure S8A), and the MK-7 yield on glucose of the strains BS20-T and BS20-Q were 0.86 mg/g and 0.83 mg/g, respectively. In addition, after 2.5 days of fermentation, the cells hardly consumed glucose in static culture, whereas glucose was consumed in shaking culture (Figure S8B). Moreover, the co-overexpression of *tatAD-CD* and *qcrA-C* in BS20 using P_{43} promoter, yielding the engineered strain BS20-QT, increased the titer of MK-7 from 360 to 410 mg/L in shake culture. We performed SDS-PAGE on whole-cell proteins of strains BS20-Q and BS20-T in shaking culture to analyze the protein abundance of the overexpression targets. The result shows that the expression of QcrA (18.74 kDa), QcrB (25.94 kDa), and QcrC (28.17 kDa) was increased compared with BS20. However, the expression of TatAD (7.43 kDa) and TatCD (27.71 kDa) did not change obviously (Figure S10), maybe due to the fact that TatAD and TatCD are membrane proteins.

Based on the above results, the engineered strain BS20-QT was further cultured in a 15-L fed-batch bioreactor for MK-7 production. In fed-batch cultivation with control of glucose concentration between 8 and 16 g/L, a total of 800 mL of feeding solution was added to the bioreactor during the culture period. As shown in Figure 7C, compared with the strain BS20, the MK-7 titer of BS20-QT was increased from 200 to 245 mg/L under the condition of low dissolved oxygen level (30%). Under the condition of high dissolved oxygen level (55%), the maximum MK-7 titer of BS20-QT in a 15-L bioreactor increased from 200 to 310 mg/L, and the maximum OD_{600} of BS20-QT was increased by 14.3% than that under the low dissolved oxygen (Figure 7D). In the early stage of fermentation, especially during the period of cell exponential growth, the dissolved oxygen level in the fermentation broth was only 5%–8% (Figure S9). These results demonstrated that fed-batch cultivation with control of high dissolved oxygen level was favorable for MK-7 production and provided a basis for large-scale production of MK-7.

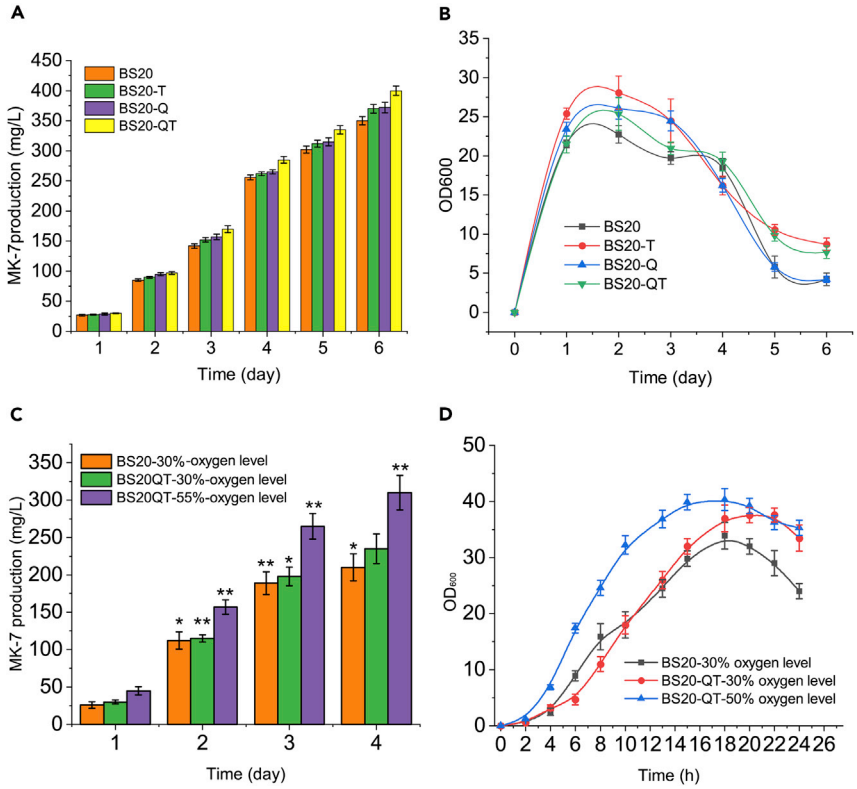

Figure 7. The Titer of MK-7 in 250 mL Flask and 15-L Bioreactor

(A) The titers of MK-7 synthesized by strains BS20, BS20-Q, BS20-T, and BS20-QT.

(B) The cell growth of BS20, BS20-Q, BS20-T, and BS20-QT.

(C) Effect of dissolved oxygen level (30% and 55%) on the synthesis of MK-7.

(D) Effect of dissolved oxygen level (30% and 55%) on cell growth. We define that when the seed is not added, the dissolved oxygen level in the fermentation broth is 100%. All experiments were independently carried out at least three times, and the results were expressed as mean ± standard deviation (SD). *$p < 0.05$ and **$p < 0.01$, respectively.

DISCUSSION

In *B. subtilis,* the robust biofilm formation requires large quantities of ferric iron to promote the production of iron-containing enzymes involved in respiratory electron transfer and establishes strong membrane potential, which is considered to be a key factor in the production of biofilm matrix (Qin et al., 2019). Fang et al. (2018) proved that the cobalt uptake transport system is essential for *de novo* vitamin B12 biosynthesis in *Escherichia coli*. Furthermore, MK-7 is a component of bacterial cell membranes and plays an important role in electron transfer, and thus, the state of cell membrane may also affect the synthesis of MK-7. Wang et al. (2019) detected the relationship between the concentration of MK-7 and the value of surface tension and found that maintaining the stable surface tension of cell membrane is beneficial to the accumulation of MK-7. Ranmadugala et al., 2017 discovered that changing the state or composition of the membrane in *B. subtilis*natto could increase the synthesis of MK-7. Herein, we found that the expression level of cell-membrane-associated proteins changed most significantly under shake culture and static culture, and further overexpressing these membrane protein genes could promote the synthesis of MK-7. These results indicate that cell membranes play a significant role in the synthesis of MK-7, which may be owing to the fact that stable state and composition of cell membrane will provide a stable synthesis and storage platform for MK7, and in return, high concentration of MK7 could ensure the efficiency of electron transfer.

OxdC can catalyze the conversion of oxalate to formate and CO_2 and then extract electrons from formate oxidation (Yang et al., 2015). The protein content of OxdC was significantly higher in static culture, which was important for electron generation. Knockout of *oxdC* did not reduce the production of MK-7, which may be because the increased expression level of NADH dehydrogenase (Figure 6G) also could maintain the concentration of electron to stabilize the efficiency of electron transfer. Previous studies showed that

the concentration of MK-7 was inversely proportional to the ratio of NADH/NAD^+ in *B. subtilis* (Wang et al., 2019). It was reported that the synthesis of coenzyme Q (transport electrons like MK-7) was promoted by increasing the NADH/NAD^+ ratio in *Rhodobactersphaeroides* (Zhu et al., 2017). The reason may be that as a Gram-positive aerobic bacterium, *B. subtilis* can only use MK-7 as the carrier of electron transport, whereas *E. coli* and *R. sphaeroides* are facultative anaerobes, which can utilize ubiquinone (CoQ-8) to transport electrons under aerobic conditions and use MK-7 when grown anaerobically. It was reported that increasing the supply of oxygen could effectively improve the synthesis of MK-7 (Berenjian et al., 2014). In this study, overexpression of *qcrA-C* increased the efficiency of electron transport to oxygen and increasing the supply of oxygen in the 15-L bioreactor was beneficial to the synthesis of MK-7. These results also confirmed that the sufficient electron transport was an important factor for efficient synthesis of MK-7.

In summary, we demonstrated that biofilm has significant effects on the MK-7 synthesis by comparative transcriptomics analysis of the strains in shake culture and static culture. Besides, we clarified that the electron transport also has remarkable influence on the synthesis of MK-7. The co-overexpression of the cell membrane components signals transduction protein *tatAD-CD* (BSU02630) and menaquinol-cytochrome c reductase *qcrA-C* in BS20 increased the MK-7 titer in 15-L bioreactor by 55% to 310 mg/L.

Limitations of the Study

Here we show the effect of cell-membrane-associated proteins and electron transport on MK-7 synthesis. The synthesis of MK-7 is also affected by temperature and pH, and the corresponding regulatory transcription factors have not been explored in this study. Further work will focus on the regulation of global transcription factors related to temperature and pH to further promote the synthesis of MK-7.

METHODS

All methods can be found in the accompanying Transparent Methods supplemental file.

SUPPLEMENTAL INFORMATION

Supplemental Information can be found online at https://doi.org/10.1016/j.isci.2020.100918.

ACKNOWLEDGMENTS

This work was financially supported by the Key Research and Development Program of China (2018YFA0900300, 2018YFA0900504), the National Natural Science Foundation of China (31622001, 31871784, 31870069, 31671845, 31930085), the Fundamental Research Funds for the Central Universities (JUSRP51713B), and Postgraduate Research & Practice Innovation Program of Jiangsu Provence (KYCX18_1786).

AUTHOR CONTRIBUTIONS

L.L., L.J., G.D. designed the research. S.C., H.X., and T.C. performed the experiments. L.L., S.C., Y.G.,Y.L., and X.L. analyzed the data. L.L., S.C., Y.G., and X.L. wrote the manuscript.

DECLARATION OF INTERESTS

The authors declare no competing interests.

Received: November 4, 2019
Revised: January 9, 2020
Accepted: February 11, 2020
Published: March 27, 2020

REFERENCES

Antelmann, H., Scharf, C., and Hecker, M. (2000). Phosphate starvation-inducible proteins of *Bacillus subtilis*: proteomics and transcriptional analysis. J. Bacteriol. *182*, 4478–4490.

Berenjian, A., Chan, N.L., Mahanama, R., Talbot, A., Regtop, H., Kavanagh, J., and Dehghani, F. (2013). Effect of biofilm formation by *Bacillus subtilis*natto on menaquinone-7 biosynthesis. Mol. Biotechnol. *54*, 371–378.

Berenjian, A., Mahanama, R., Kavanagh, J., and Dehghani, F. (2015). Vitamin k series: current status and future prospects. Crit. Rev. Biotechnol. *35*, 199–208.

Berenjian, A., Mahanama, R., Talbot, A., Biffin, R., Regtop, H., Valtchev, P., Kavanagh, J., and Dehghani, F. (2011). Efficient media for high menaquinone-7 production: response surface

methodology approach. Nat. Biotechnol. *28*, 665–672.

Berenjian, A., Mahanama, R., Talbot, A., Regtop, H., Kavanagh, J., and Dehghani, F. (2012). Advances in menaquinone-7 production by *Bacillus subtilis*natto: fed-batch glycerol addition. Am. J. Biochem. Biotechnol. *8*, 105–110.

Berenjian, A., Mahanama, R., Talbot, A., Regtop, H., Kavanagh, J., and Dehghani, F. (2014). Designing of an intensification process for biosynthesis and recovery of menaquinone-7. Appl. Biochem. Biotechnol. *172*, 1347–1357.

Branda, S.S., Chu, F., Kearns, D.B., Losick, R., and Kolter, R. (2006). A major protein component of the *Bacillus subtilis* biofilm matrix. Mol. Microbiol. *59*, 1229–1238.

Cairns, L.S., Hobley, L., and Stanley-Wall, N.R. (2014). Biofilm formation by *Bacillus subtilis*: new insights into regulatory strategies and assembly mechanisms. Mol. Microbiol. *93*, 587–598.

Chu, F., Kearns, D.B., Branda, S.S., Kolter, R., and Losick, R. (2006). Targets of the master regulator of biofilm formation in *Bacillus subtilis*. Mol. Microbiol. *59*, 1216–1228.

Conter, C., Oppici, E., Dindo, M., Rossi, L., Magnani, M., and Cellini, B. (2019). Biochemical properties and oxalate-degrading activity of oxalate decarboxylase from *Bacillus subtilis* at neutral ph. IUBMB Life *71*, 917–927.

Cui, S., Lv, X., Wu, Y., Li, J., Du, G., Ledesma-Amaro, R., and Liu, L. (2019). Engineering a bifunctional phr60-rap60-spo0a quorum-sensing molecular switch for dynamic fine-tuning of menaquinone-7 synthesis in *Bacillus subtilis*. ACS Synth. Biol. *8*, 1826–1837.

Diehl, A., Roske, Y., Ball, L., Chowdhury, A., Hiller, M., Moliere, N., Kramer, R., Stoppler, D., Worth, C.L., Schlegel, B., et al. (2018). Structural changes of tasa in biofilm formation of *Bacillus subtilis*. Proc. Natl. Acad. Sci. U S A *115*, 3237–3242.

Fang, H., Li, D., Kang, J., Jiang, P., Sun, J., and Zhang, D. (2018). Metabolic engineering of *Escherichia coli* for de novo biosynthesis of vitamin B12. Nat. Commun. *9*, 4917.

Glaser, P., Danchin, A., Kunst, F., Zuber, P., and Nakano, M.M. (1995). Identification and isolation of a gene required for nitrate assimilation and anaerobic growth of *Bacillus subtilis*. J. Bacteriol. *177*, 1112–1115.

Grober, U., Reichrath, J., Holick, M.F., and Kisters, K. (2014). Vitamin k: an old vitamin in a new perspective. Dermatoendocrinol *6*, e968490.

Iwamoto, J. (2014). Vitamin k(2) therapy for postmenopausal osteoporosis. Nutrients *6*, 1971–1980.

Kobayashi, K., and Iwano, M. (2012). Bsla(yuab) forms a hydrophobic layer on the surface of *Bacillus subtilis* biofilms. Mol. Microbiol. *85*, 51–66.

Kolodkin-Gal, I., Elsholz, A.K., Muth, C., Girguis, P.R., Kolter, R., and Losick, R. (2013). Respiration control of multicellularity in *Bacillus subtilis* by a complex of the cytochrome chain with a membrane-embedded histidine kinase. Genes Dev. *27*, 887–899.

Liu, W., Li, S., Wang, Z., Yan, E.C.Y., and Leblanc, R.M. (2017). Characterization of surface-active biofilm protein bsla in self-assembling Langmuir monolayer at the air-water interface. Langmuir *33*, 7548–7555.

Lyons, J.A., Aragao, D., Slattery, O., Pisliakov, A.V., Soulimane, T., and Caffrey, M. (2012). Structural insights into electron transfer in caa3-type cytochrome oxidase. Nature *487*, 514–518.

Mahanama, R., Berenjian, A., Valtchev, P., Talbot, A., Biffin, R., Regtop, H., Dehghani, F., and Kavanagh, J.M. (2011). Enhanced production of menaquinone 7 via solid substrate fermentation from Bacillus subtilis. Int. J. Food Eng. *7*, 1–23.

Mahdinia, E., Demirci, A., and Berenjian, A. (2018). Implementation of fed-batch strategies for vitamin k (menaquinone-7) production by *Bacillus subtilis*natto in biofilm reactors. Appl. Microbiol. Biotechnol. *102*, 9147–9157.

Mielich-Suss, B., and Lopez, D. (2015). Molecular mechanisms involved in *Bacillus subtilis* biofilm formation. Environ. Microbiol. *17*, 555–565.

Qin, Y., He, Y., She, Q., Larese-Casanova, P., Li, P., and Chai, Y. (2019). Heterogeneity in respiratory electron transfer and adaptive iron utilization in a bacterial biofilm. Nat. Commun. *10*, 3702.

Que, Q., and Helmann, J.D. (2000). Manganese homeostasis in *Bacillus subtilis* is regulated by mntR, a bifunctional regulator related to the diphtheria toxin repressor family of proteins. Mol. Microbiol. *35*, 1454–1468.

Ranmadugala, D., Ebrahiminezhad, A., Manley-Harris, M., Ghasemi, Y., and Berenjian, A. (2017). Impact of 3-aminopropyltriethoxysilane-coated iron oxide nanoparticles on menaquinone-7 production using B. subtilis. Nanomaterials (Basel) *7*, 350.

Ravishankar, B., Dound, Y.A., Mehta, D.S., Ashok, B.K., de Souza, A., Pan, M.-H., Ho, C.-T., Badmaev, V., and Vaidya, A.D.B. (2015). Safety assessment of menaquinone-7 for use in human nutrition. J. Food Drug Anal. *23*, 99–108.

Romero, D., Aguilar, C., Losick, R., and Kolter, R. (2010). Amyloid fibers provide structural integrity to *Bacillus subtilis* biofilms. Proc. Natl. Acad. Sci. U S A *107*, 2230–2234.

Sato, T., Schurgers, L.J., and Uenishi, K. (2012). Comparison of menaquinone-4 and menaquinone-7 bioavailability in healthy women. Nutr. J. *11*, 93.

Song, Y., Nikoloff, J.M., and Zhang, D. (2015). Improving protein production on the level of regulation of both expression and secretion pathways in *Bacillus subtilis*. J. Microbiol. Biotechnol. *25*, 963–977.

Wang, H., Liu, H., Wang, L., Zhao, G., Tang, H., Sun, X., Ni, W., Yang, Q., Wang, P., and Zheng, Z. (2019). Improvement of menaquinone-7 production by *Bacillus subtilis*natto in a novel residue-free medium by increasing the redox potential. Appl. Microbiol. Biotechnol. *103*, 7519–7535.

Wilks, J.C., Kitko, R.D., Cleeton, S.H., Lee, G.E., Ugwu, C.S., Jones, B.D., BonDurant, S.S., and Slonczewski, J.L. (2009). Acid and base stress and transcriptomic responses in *Bacillus subtilis*. Appl. Environ. Microbiol. *75*, 981–990.

Wu, W.-J., and Ahn, B.-Y. (2011). Improved menaquinone (vitamin k2) production in cheonggukjang by optimization of the fermentation conditions. Food Sci. Biotechnol. *20*, 1585–1591.

Yang, S., Cao, Y., Sun, L., Li, C., Lin, X., Cai, Z., Zhang, G., and Song, H. (2019). Modular pathway engineering of *Bacillus subtilis* to promote de novo biosynthesis of menaquinone-7. ACS Synth. Biol. *8*, 70–81.

Yang, Y., Wu, Y., Hu, Y., Cao, Y., Poh, C.L., Cao, B., and Song, H. (2015). Engineering electrode-attached microbial consortia for high-performance xylose-fed microbial fuel cell. ACS Catal. *5*, 6937–6945.

Yepes, A., Schneider, J., Mielich, B., Koch, G., Garcia-Betancur, J.C., Ramamurthi, K.S., Vlamakis, H., and Lopez, D. (2012). The biofilm formation defect of a *Bacillus subtilis*flotillin-defective mutant involves the protease ftsh. Mol. Microbiol. *86*, 457–471.

Yu, J., Hederstedt, L., and Piggot, P.J. (1995). The cytochrome bc complex (menaquinone:Cytochrome c reductase) in *Bacillus subtilis* has a nontraditional subunit organization. J. Bacteriol. *177*, 6751–6760.

Zhu, Y., Ye, L., Chen, Z., Hu, W., Shi, Y., Chen, J., Wang, C., Li, Y., Li, W., and Yu, H. (2017). Synergic regulation of redox potential and oxygen uptake to enhance production of coenzyme q10 in rhodobactersphaeroides. Enzyme Microb. Technol. *101*, 36–43.

iScience, Volume *23*

Supplemental Information

Cell Membrane and Electron Transfer Engineering for Improved Synthesis of Menaquinone-7 in *Bacillus subtilis*

Shixiu Cui, Hongzhi Xia, Taichi Chen, Yang Gu, Xueqin Lv, Yanfeng Liu, Jianghua Li, Guocheng Du, and Long Liu

Supplemental Information

Supplementary Figures

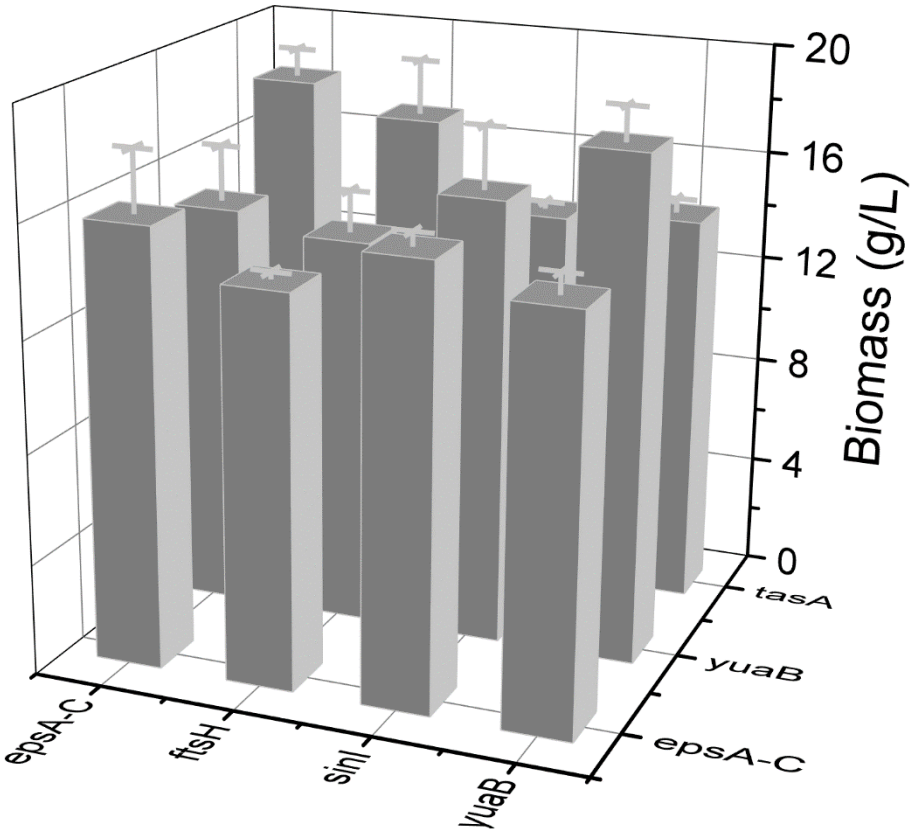

Figure S1. The effect of double knockout of biofilm-forming genes on cell biomass. All experiments were independently carried out at least three times and the results were expressed as mean ± standard deviation (SD). Related to Figure 2.

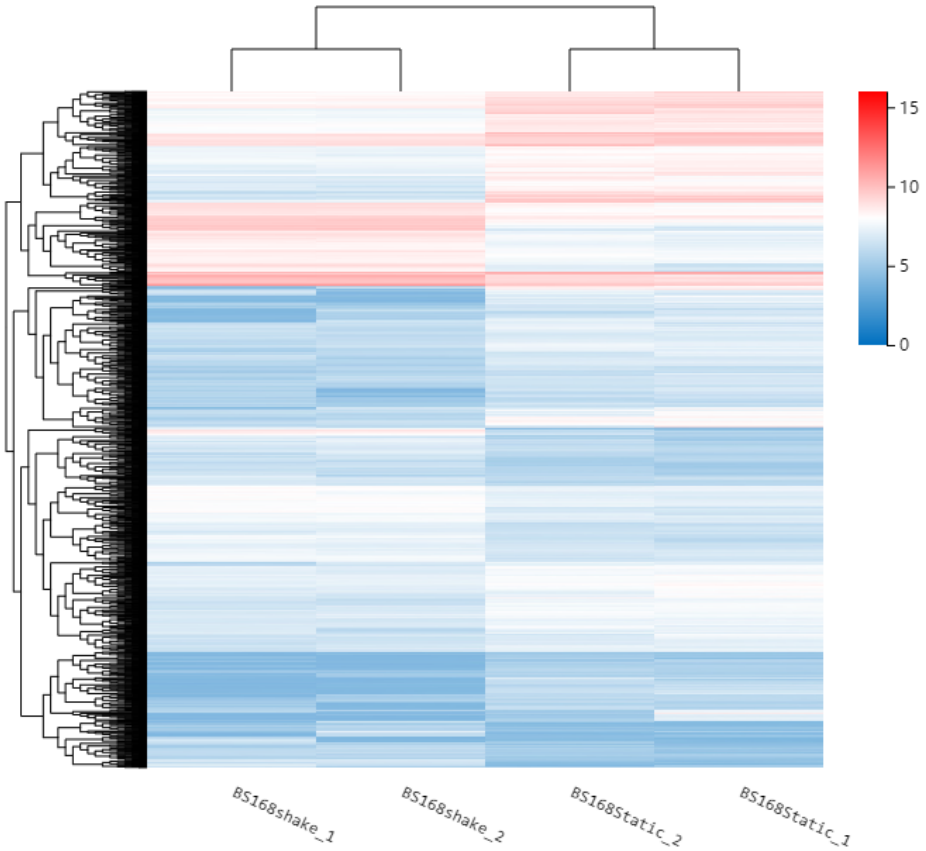

Figure S2. Heat maps show differential genes in static culture and shake cultures. Related to Figure 3 and Figure 4.

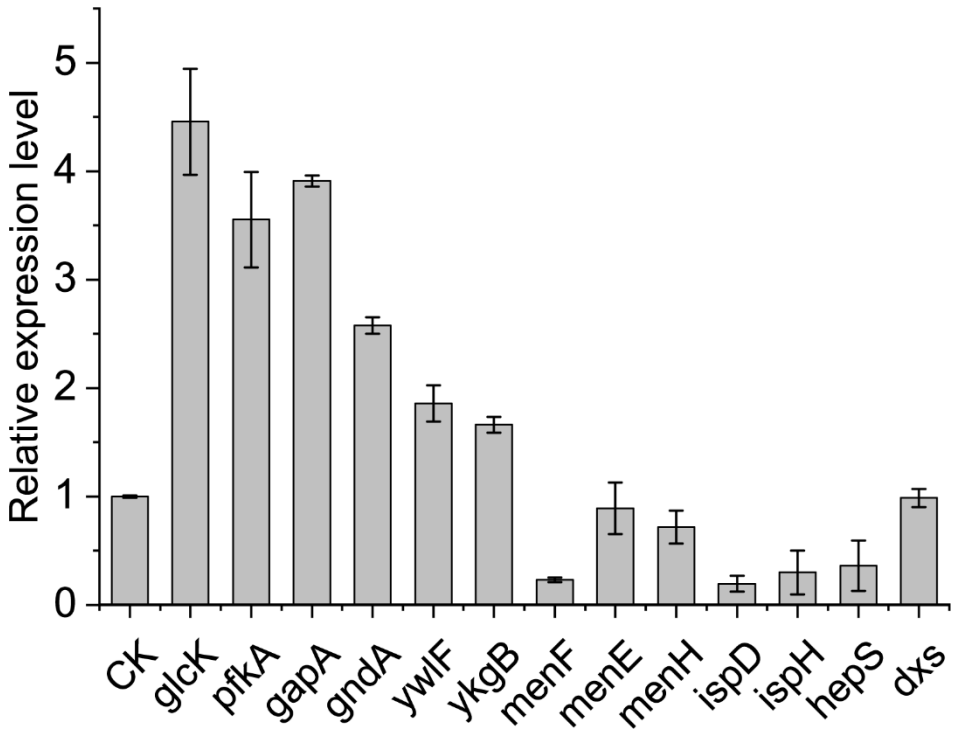

Figure S3. Relative expression levels of key genes in the glycolytic pathway, the pentose phosphate pathway, the shikimic acid pathway, the 2-C-methyl-D-erythritol-4-phosphate (MEP) pathway and MK-7 synthesis pathway. All experiments were independently carried out at least three times and the results were expressed as mean ± standard deviation (SD). Related to Figure 3.

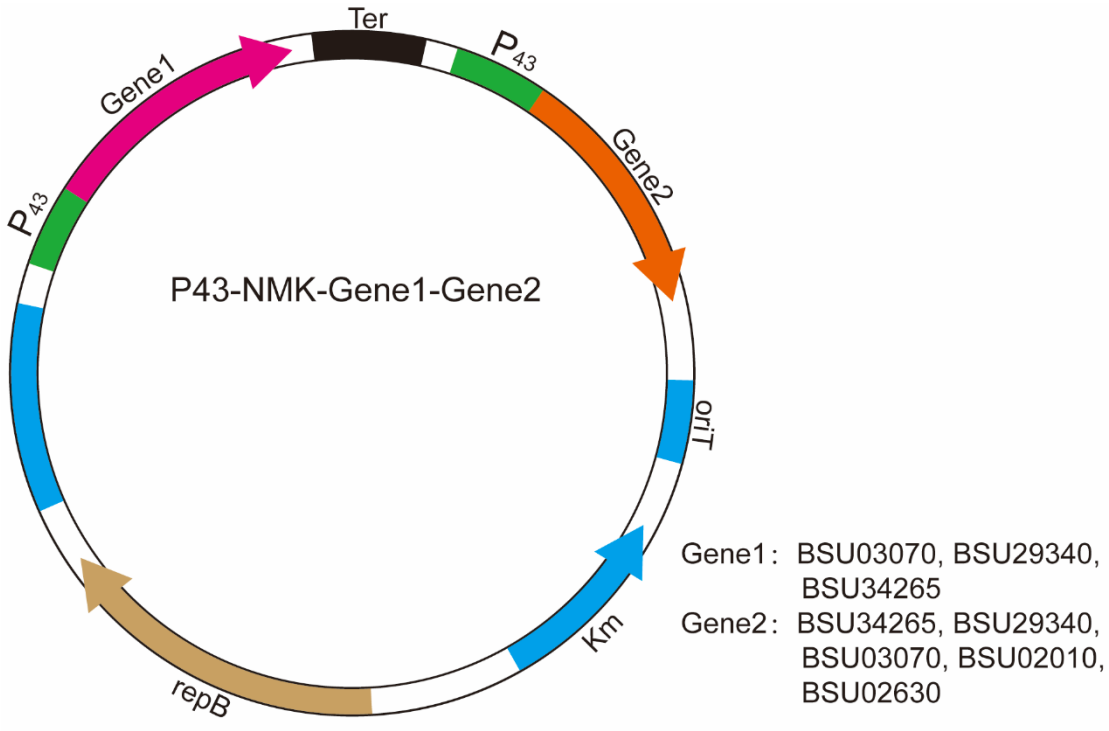

Figure S4. The plasmid map of co-expressing differential genes. Related to Figure 5.

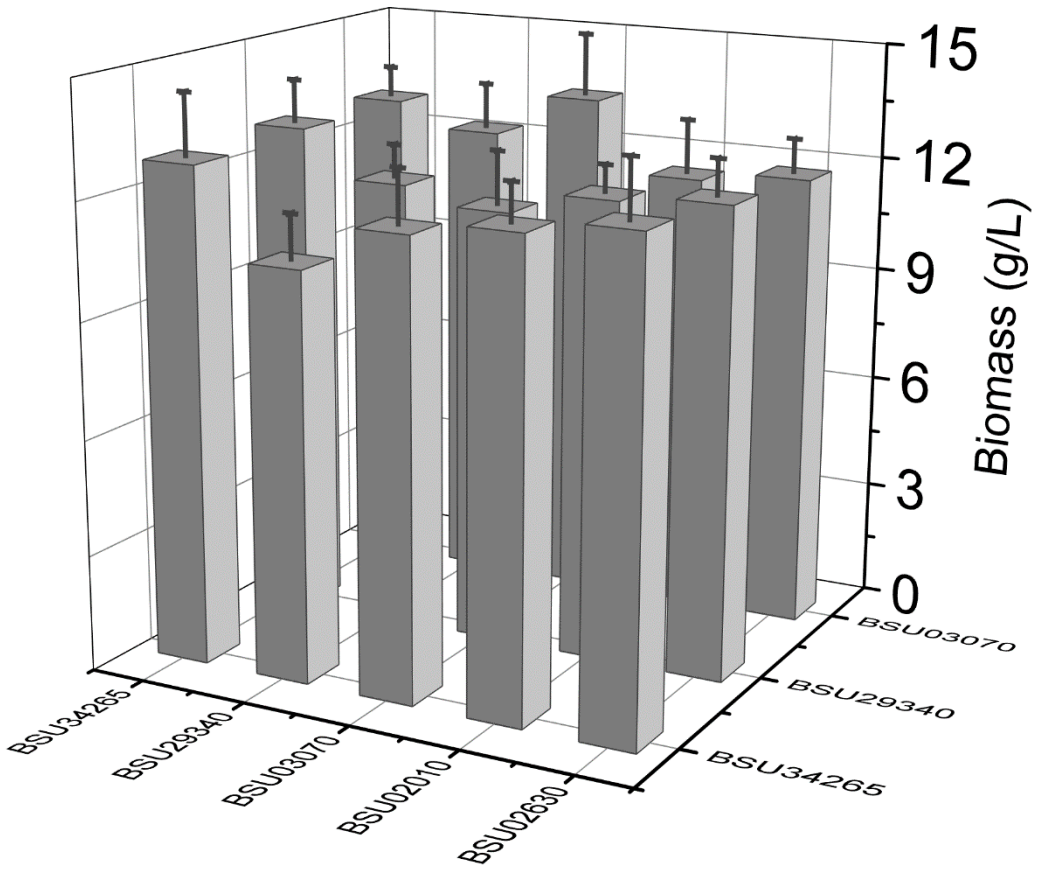

Figure S5. Effect of co-expressing differential genes on cell biomass in *Bacillus subtilis* 168. All experiments were independently carried out at least three times and the results were expressed as mean ± standard deviation (SD). Related to Figure 5.

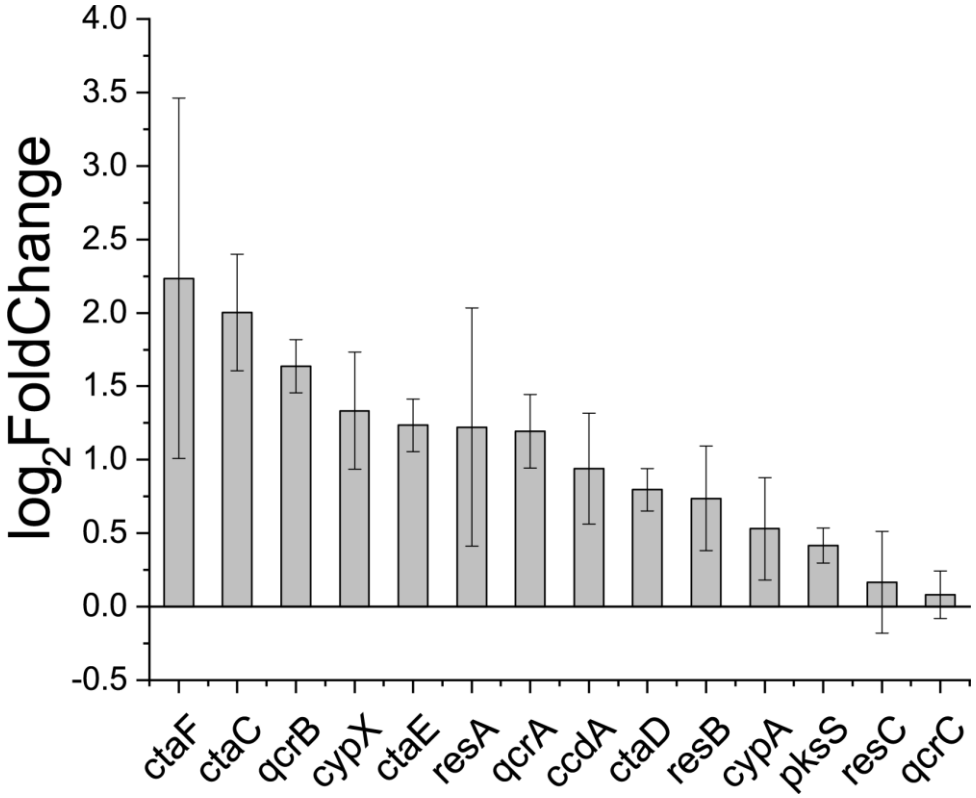

Figure S6. Gene expression levels of cytochrome genes in static culture compared to shaking culture. All experiments were independently carried out at least three times and the results were expressed as mean ± standard deviation (SD). Related to Figure 6.

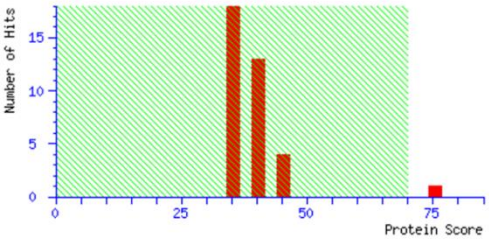

Protein sequence coverage: 31%

Matched peptides shown in ***bold red***.

```
  1 MKKQNDIPQP IRGDKGATVK IPRNIERDRQ NPDMLVPPET DHGTVSNMKF
 51 SFSDTHNRLE KGGYAREVTV RELPISENLA SVNMRLKPGA IRELHWHKEA
101 EWAYMIYGSA RVTIVDEKGC SFIDDVGEGD LWYFPSGLPH SIQALDEGAE
151 FLLVFDDGSF SENSTFQLTD WLAHTPKEVI AANFGVTKEK IANLPGKEKY
201 IFETQIPGSL KDDIVEGPNG EVPYPFTYRL LEQEPIESEG GKVYIADSTN
251 FTVSKTIASA LVTVEPGAMR ELHWHPNTHE WQYYISGKAR MTVFASDGHA
301 RTFNYQAGDV GYVPFAMGHY VENIGDEPLV FLEIFKDDHY ADVSLNQWLA
351 MLPEKFVQAH LDLGKDFTDV LSKVKHPVVK KKCSK
```

Query	Start - End	Observed	Mr(expt)	Mr(calc)	ppm	M	Score	Peptide
11	4 - 15	1380.6866	1379.6794	1379.7157	-26.3	1		K.QNDIPQPIRGDK.G
20	28 - 49	2513.1210	2512.1138	2512.1322	-7.36	1		R.DRQNPDMLVPPETDHGTVSNMK.F + 2 Oxidation (M)
2	50 - 58	1110.4659	1109.4586	1109.4890	-27.4	0		K.FSFSDTHNR.L
13	50 - 61	1480.6900	1479.6827	1479.7106	-18.9	1		K.FSFSDTHNRLEK.G
18	72 - 85	1572.7667	1571.7595	1571.7977	-24.3	0		R.ELPISENLASVNMR.L
19	72 - 85	1588.7711	1587.7638	1587.7926	-18.1	0		R.ELPISENLASVNMR.L + Oxidation (M)
1	93 - 98	849.4111	848.4038	848.4293	-30.1	0		R.ELHWHK.E
16	99 - 111	1546.6746	1545.6673	1545.6922	-16.1	0		K.EAEWAYMIYGSAR.V
17	99 - 111	1562.6837	1561.6764	1561.6871	-6.86	0		K.EAEWAYMIYGSAR.V + Oxidation (M)
21	200 - 229	3444.7699	3443.7626	3443.6925	20.3	1		K.YIFETQIPGSLKDDIVEGPNGEVPYPFTYR.L
7	291 - 301	1191.5252	1190.5179	1190.5502	-27.2	0		R.MTVFASDGHAR.T
8	291 - 301	1207.5210	1206.5137	1206.5452	-26.1	0		R.MTVFASDGHAR.T + Oxidation (M)

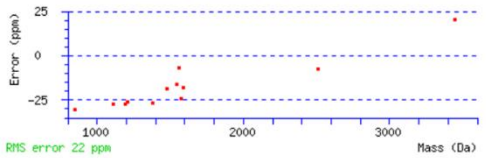

Figure S7. Protein flight mass spectrometry of oxalate decarboxylase. Related to Figure 6.

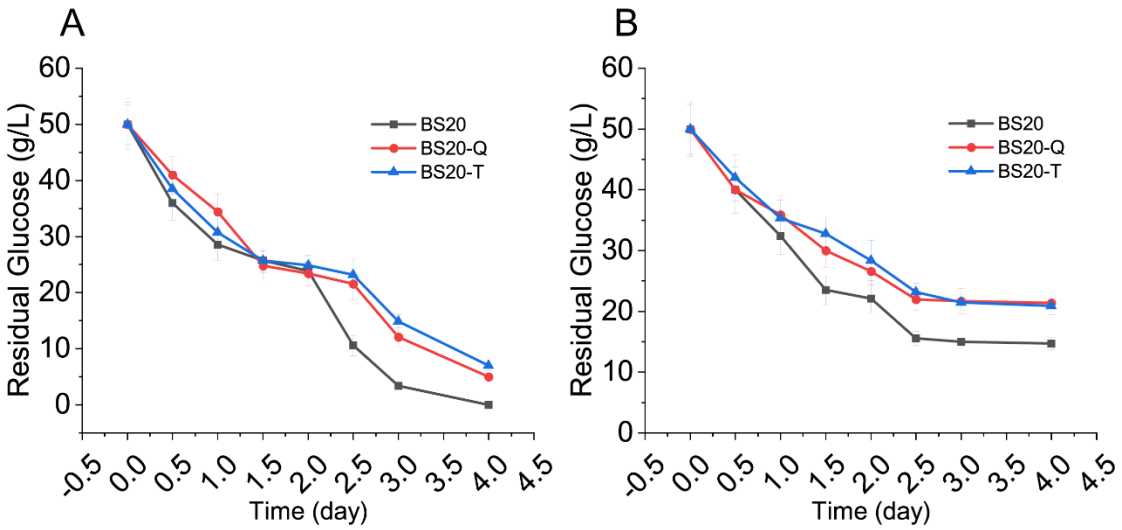

Figure S8. Time profiles of residual glucose in strains. A, The residual glucose of strains BS20, BS20-Q and BS20-T in shaking culture. B, The residual glucose of strains BS20, BS20-Q and BS20-T in static culture. All experiments were independently carried out at least three times and the results were expressed as mean ± standard deviation (SD). Related to Figure 7.

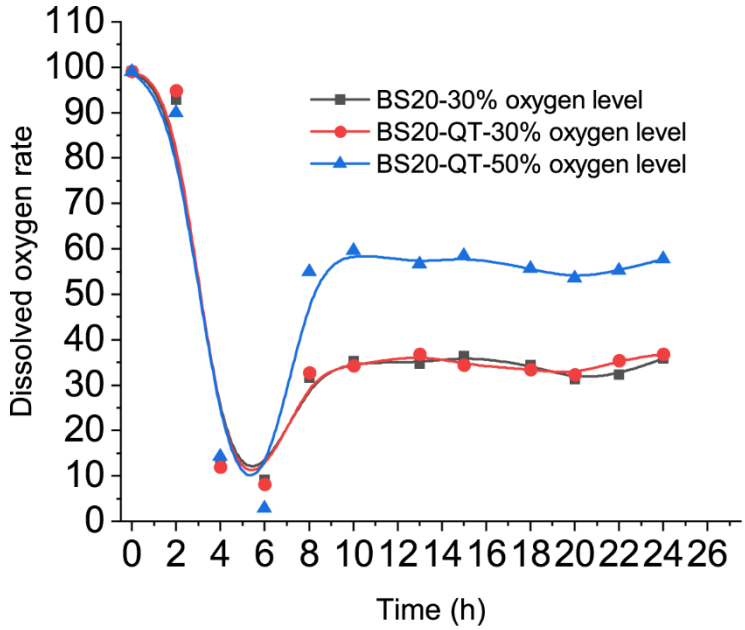

Figure S9. The oxygen content in the 15-L bioreactor. The cell density reaches the maximum, the dissolved oxygen increases continuously by controlling stirring, and stabilizes at about30% and 55%. Related to Figure 7.

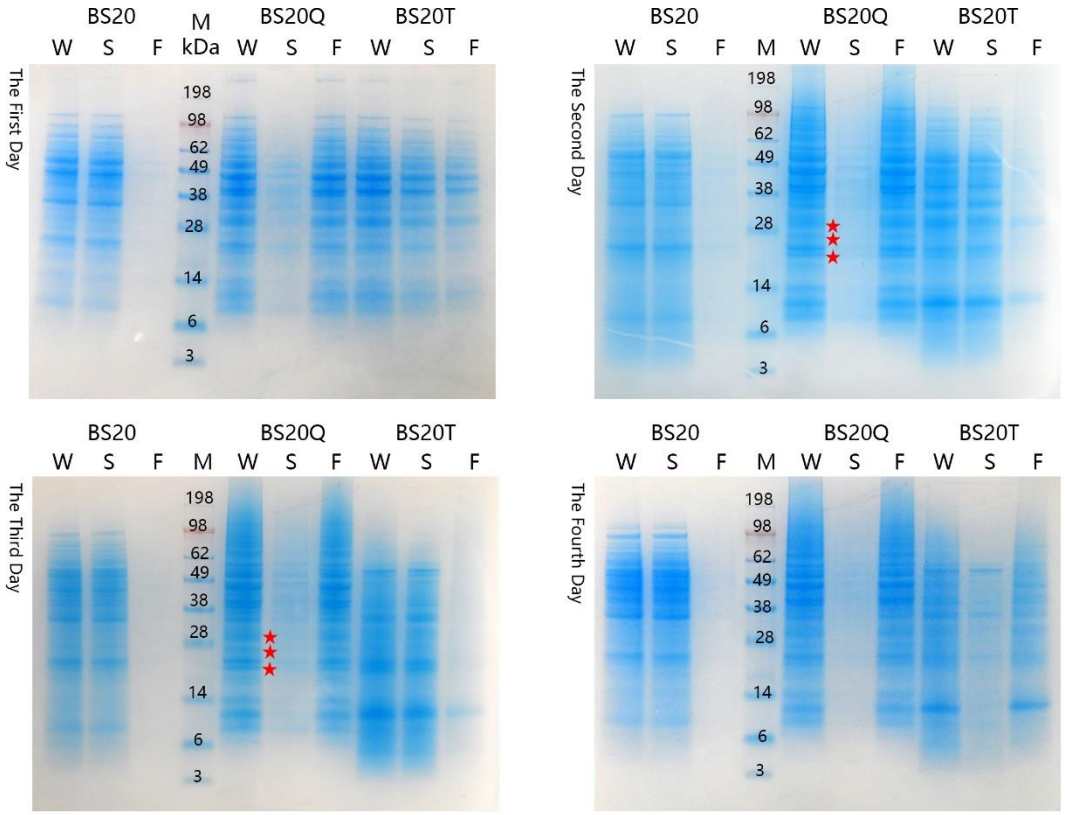

Figure S10. Protein abundance of the over-expression targets in the engineered strains. W: Whole cell, S: Supernatant after sonication and centrifugation, F: Cell debris after sonication. M: Protein standard marker. Red stars indicate target protein. Related to Figure 7.

Supplementary Tables

Table S1 Summary of transcriptome sequencing data. Related to Figure 4.

Parameter	Shaking culture	Static culture
Total number of reads (Mb)	17.96	17.96
Total clean reads (Mb)	16.01	14.91
Clean reads ratio (%)	89.15	82.95
Clean reads Q20	99.00	99.14
Clean reads Q30	96.90	97.51
FPKM<=1 gene number[a]	30	70
FPKM1-10 gene number[b]	516	689
FPKM>=10 gene number[c]	3047	3180

a FPKM <= 1 is a gene with very low expression level

b. FPKM1-10 is a gene with a lower expression level

c FPKM>=10 is a gene with a medium and high expression level

Table. S6 The genes with distinct expression differences. Related to Figure 4.

NO.	Gene ID	Gene alias	molecular function	Local	log2 (BS168Static/CK)
1	BSU01910	skfA	response to stimulus	extracellular region	8.76
2	BSU30760	mntB	small molecule binding	plasma membrane	7.36
3	BSU02010	ybdK	signaling receptor and transducer	intracellular	5.68
4	BSU05410	ydfH	signaling receptor activity	Intracellular; plasma membrane	5.42
5	BSU29340	tcyN	transmembrane transporter activity	Plasma membrane	7.32
6	BSU08840	ssuA	transmembrane transporter activity	plasma membrane	11.32
7	BSU02000	ybdJ	intracellular signal transduction	cytoplasm	8.20
8	BSU03070	mdr	transmembrane transporter activity	plasma membrane	4.58
9	BSU13610	mtnB	Cation binding	intracellular	7.72
10	BSU36660	ureA	cation binding	cytoplasm	4.43
11	BSU02630	tatAD	peptide transporter activity	plasma membrane	6.20
12	BSU03200	putB	cofactor binding; oxidoreductase activity	intracellular	5.37
13	BSU34265	epsK	polysaccharide metabolic process	plasma membrane	8.17
14	BSU24640	tapA		membrane	7.92

Transparent Methods

Bacterial strains and growth conditions.

The wild-type strain *Bacillus subtilis* 168 was used as the control strain for MK-7 synthesis. All strains were cultivated in Lysogeny Broth (LB) liquid culture or on LB agar plates at 37°C for genetic experiments. The fermentation medium consisted of 5% (w/v) glucose, 5% (w/v) sucrose, 5% (w/v) soy peptone, and 0.06% (w/v) KH_2PO_4. Glucose and sucrose are separately sterilized for 15 min at 115°C, and the other components were sterilized for 30 min at 121°C. Appropriate antibiotics were added to the medium: ampicillin (100 μg/mL), zeocin (20 μg/mL), kanamycin (50 μg/mL), chloramphenicol (5 μg/mL), and spectinomycin (50 μg/mL). All chemicals were purchased from Sangon Biotech Co., Ltd (Shanghai, China). MK-7 standard was purchased from ChromaDex (Irvine, CA, USA). Soy peptone, glycerol, and glucose were purchased from Sinopharm Chemical Reagent Co., Ltd (shanghai, China). Methanol, dichloromethane, 2-propanol, and n-hexane were obtained from Sigma-Aldrich (St. Louis, MO, USA).

Static culture and biofilm quantification of the engineered *B. subtilis.*

The engineered *B. subtilis* strains were grown in 3 mL LB at 37°C with shaking at 220 rpm for 15 h in a 15-mL tube. A seed culture (0.1 mL) was inoculated into a 12-well plate containing 4 mL of fermentation medium and grown at 40°C for 4 days. To ensure the consistency of biofilm biomass with MK-7 production, the biofilm was resuspended in the fermentation broth by shaking, and then divided into two parts, one for detecting the concentration of MK-7, and the other was used for biofilm collection after centrifugation. The filter paper was used to remove excess fermentation liquid, and the biomass of the biofilm was weighed.

Transcriptome analysis and gene expression analysis

B. subtilis 168 was cultured in the fermentation medium in 250 ml flasks with 20 ml fermentation medium and grown at 40°C with shaking at 220 rpm for 3 days. The cultured conditions were static under the same conditions without shaking. The total RNA of these strains was extracted, synthetic the first cDNA and DNA sequencing were performed on a HiSeq 2500sequencing system By the Beijing Genomics Institute (BGI, Wuhan, China). Gene-level statistics for shake versus static culture were calculated using the DESeq2 program with default parameters, and differentially expressed genes were identified based on an adjusted P value < 0.05. Downstream functional classification was achieved by gene ontology (GO) enrichment analysis and Kyoto Encyclopedia of Genes and Genomes (KEGG) pathway analysis. Quantitative reverse-transcriptase PCR (qRT-PCR) was applied to verify the RNA-seq results, the 16S rRNA gene was used as an internal standard.

B. subtilis transformation, DNA assembly and plasmid construction.

DNA constructs and plasmid construction were generated using previously described assembly methods and transformed into *B. subtilis* by electroporation. The plasmids were sequenced by GENEWIZ (South Plainfield, NJ, USA).

NADH and NAD^+ analysis

NADH and NAD^+ levels of *B. subtilis* and BS20 were measured using a commercially available

kit (cominbio, china) according to the manufacturer`s instructions. NADH and NAD^+ levels were quantified by a colorimetric assay at 570 nm. The level of NADH and NAD^+ were calculated with per unit cell density OD_{600}.

MK-7 extraction and analytical methods.

The biofilm and fermentation liquid were sampled for MK-7 concentration analysis. MK-7 was extracted from the fermentation supernatant and cell precipitate using a mixture of 2-propanol and *n*-hexane (1:2, v/v) in a 4:1 ratio (organic:liquid, v/v). The mixture was vigorously shaken with a vortex mixer for 10 min and then centrifuged at 5,000 × *g* for 5 min to separate the two phases. The organic phase was then separated to recover the extracted MK-7. High-performance liquid chromatography (Agilent 1260, Santa Clara, CA, USA) equipped with a photon diode array UV detector and C18 ODS column (5 μm, 250 × 4.6 mm, Thermo Fisher Scientific, Waltham, MA, USA) was used at 40°C to determine the MK-7 concentration. Methanol: dichloromethane (9:1, v/v) was used as the mobile phase at a flow rate of 1 mL/min. A wavelength of 254 nm was used for calibration and analysis. The MK-7 calibration curve was linear between 20 mg/L and 300 mg/L (R^2 = 0.998).

To analyze the protein by SDS-PAGE, the sample was broken with sonication for a total of 10 minutes, ultrasonically for 2s, and still for 2s. The experiment was performed on a 10% running gel in MES (morpholineethanesulfonic acid) SDS running buffer (Bio-Rad Laboratories, Hercules, CA, USA). The gel was dyed by Coomassie brilliant blue G250 to visualize the proteins.

Fed-Batch culture in 250 ml flask and 15-L bioreactor.

Shake-flask culture for the production of MK-7: 0.6 mL of seed solution cultured for 12 h in LB was added to baffled 250 mL shake flask with 15 mL of fermentation medium. Fermentation conditions are 40 °C, 220 rpm. 0.5 mL samples were taken during fermentation for detected the titer of MK-7.

The production of MK-7 by fed-batch culture of BS20-QT was performed at an initial glucose concentration of 10 g/L. The fermentation medium used for fed-batch culture consisted of 50 g/L soy peptone, 5 g/L glucose, 5 g/L sucrose and 0.6 g/L KH_2PO_4. The feeding solution contained 500 g/L glucose and 500 g/L sucrose. Seed culture was carried out in 2 L shake flasks containing 500 mL of seed medium with shaking at 220 rpm and 37 °C for 12 h on rotary shakers. The seed culture was inoculated into 15-L fermenter containing 10 L fermentation medium. The pH was natural, and the temperature was maintained at 40 °C. The aeration rate and agitation speed were 10 vvm and 500 rpm, respectively. In fed-batch culture, whenever the residual glucose concentration fell to lower than 5 g/L, the feeding solution was pumped into the fermenter to restore the glucose concentration to 3-6 g/L. The feeding rates were adjusted every 2 h based on the concentration of residual glucose in the fermentation medium.

Statistical analysis. All experiments were independently carried out at least three times and the results were expressed as mean ± standard deviation (SD). Statistical data analysis was performed with *t*-texts in SPSS 25.0. P values of <0.05 were considered statistically significant, and statistical significance is indicated as * for $p < 0.05$ and ** for $p < 0.01$.

Data and Software Availability

The transcriptomics project has been deposited in the NCBI under the BioProject (https://www.ncbi.nlm.nih.gov/bioproject) accession PRJNA599448. The sequencing data have been deposited in NCBI Sequence Read Archive (SRA; https://www.ncbi.nlm.nih.gov/sra) under the accession numbers of SRR10850408, SRR10850407, SRR10850406, SRR10850405, SRR10850404, SRR10850403, SRR10850402, SRR10850401.